Temperature and melting of laser-shocked iron releasing into an LiF window

G. Huser, M. Koenig, A. Benuzzi-Mounaix, E. Henry, T. Vinci, B. Faral, M. Tomasini, B. Telaro, and D. Batani

Citation: Physics of Plasmas **12**, 060701 (2005); doi: 10.1063/1.1896375
View online: http://dx.doi.org/10.1063/1.1896375
View Table of Contents: http://scitation.aip.org/content/aip/journal/pop/12/6?ver=pdfcov
Published by the AIP Publishing

Temperature and melting of laser-shocked iron releasing into an LiF window

G. Huser,[a] M. Koenig, A. Benuzzi-Mounaix, E. Henry, T. Vinci, and B. Faral
Laboratoire pour l'Utilisation des Lasers Intenses (LULI), Ecole Polytechnique, 91128 Palaiseau, France

M. Tomasini, B. Telaro, and D. Batani
Dipartimento di Fisica, Università degli Studi di Milano, Bicocca and INFM, piazza della Scienza 3, 20126 Milano, Italy

(Received 10 September 2004; accepted 28 February 2005; published online 27 May 2005)

Absolute reflectivity and self-emission diagnostics are used to determine the gray-body equivalent temperature of laser-shocked iron partially releasing into a lithium fluoride window. Pressure and reflectivity are measured simultaneously by means of velocity interferometer system for any reflector interferometers. In the temperature-pressure plane, a temperature plateau in the release is observed which is attributed to iron's melting line. Extrapolation of data leads to a melting temperature at Earth's inner-outer core boundary of 7800 ± 1200 K, in good agreement with previous works based on dynamic compression. Shock temperatures were calculated and found to be in the liquid phase. © *2005 American Institute of Physics*. [DOI: 10.1063/1.1896375]

The locus of the iron melting line at megabar pressures is an essential factor for the description of the Earth's core thermodynamics. Namely, it is a parameter of crucial importance for expressing the energy released by the solid inner core when crystallizing at 3.3 Mbar into the liquid outer core. This problem is still at the center of a long standing controversy and no consensus has clearly been established yet. Static measurements of phase boundaries and the melting line can be achieved with good precision[1–4] but need to be extrapolated above about 1 Mbar. The use of dynamic compression techniques is therefore necessary to overcome this limit.

Shock temperature is often calculated using thermodynamics and assumed values of heat capacity and of the Grüneisen parameter.[5,6] Indeed, temperature has always been the most difficult parameter to determine in experiments involving opaque materials. Due to the short time scales of the involved phenomena, only optical pyrometry allows a direct measurement. Previous works on shocked iron temperature measurements performed with gas guns may have in principle limitations.[7,8] In those experiments indeed, shock pressure is deduced from impactor speed and impedance mismatch, while temperature is given by a blackbody fit to the radiation emitted by the sample/window material interface. The inertia of the impactor allows the shock pressure to be maintained for typically 100 ns and provides a good precision for mechanical parameters such as shock speed. However, thermal transfer of the iron sample to the window material has to be considered with these time scales, as it lowers the interface blackbody radiation.

In this paper we describe an experiment in which a slowly decaying shock was launched into an iron sample tamped by a lithium fluoride (LiF) window material using high power laser beams. When the shock is transmitted into the LiF window, the latter is compressed in a nearly hydrostatic way[9] and the interface moves at the released particle velocity in Fe which decreases with time. An entire range of pressure was therefore spanned on a same shot. The time scales involved are much shorter than with a gas gun, so that thermal transfer issues can completely be neglected.

Simultaneous measurements of time-resolved interface velocity, absolute reflectivity and self-emission enabled us to determine the pressure variation with temperature for iron release states into LiF. In particular, we observed a temperature plateau in the 0.5–1.5 Mbar range, which can be attributed to the crossing of iron's melting line.

Experiments have been performed using three of the six available beams of the LULI Nd-glass laser (converted at $\lambda = 0{,}527$ μm with a maximum total energy $E_{2\omega} \approx 100$ J) focused on a same focal spot with a ≈ 250 μm diameter flat region at the center. The laser temporal profile was a square with a rise time of 120 ps giving a full width at half maximum of 720 ps. Targets were made of 15 μm of iron tamped by 80–400 μm thick LiF substrates.

The diagnostics consisted of two VISAR (velocity interferometer system for any reflector) interferometers[10] to resolve 2π fringe shift ambiguities and of self-emission coupled to a streak camera (Fig. 1).

The two VISAR interferometers worked at 532 and 1064 nm wavelength and with sensitivities 3.4 and 16.7 km/s/frings, respectively. This allowed measurements of time-resolved interface velocity,[11] as well as absolute, dual-wavelength reflectivity. The latter were performed using intensity fiducial beams, made of 200 μm core diameter fiber optics relaying the probe Nd:YAG (YAG—yttrium aluminum garnes) laser to the slit of the streak camera. This system was first calibrated using a mirror of known reflectivity (95%) positioned in the place of the sample rear surface. Absolute reflectivity could then be deduced from the ratio of fringe to fiducial intensities on the sample material (Fig. 2).

Reflectivity was used in conjunction with self-emission

[a]Present address: Commissariat à l'Energie Atomique (CEA), BP 12, 91680 Bruyères-le-Chatel, France. Electronic mail: gael.huser@cea.fr

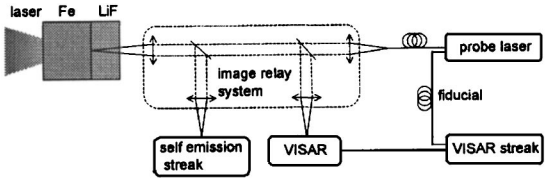

FIG. 1. Schematic view of the experimental setup.

data in order to determine the radiating Fe/LiF interface greybody equivalent temperature. Reflectivity data were corrected from Fresnel losses at LiF/vacuum and LiF/compressed LiF interfaces. The latter were found not to exceed a few percent. Reflectivities at shock breakout (~0.5 at 532 nm and ~0.6 at 1064 nm) were below their standard values, which is not surprising for a highly heated metal. The reflectivity spectrum in the visible range was taken to be flat from the 532 nm experimental value, as no interband transitions are expected to have a significant effect, given the uncertainties (a few percent).

A careful self-emission calibration procedure was achieved in order to link the number of counts recorded on the CCD (charge coupled device) to the actual emitting interface temperature. The CCD/streak camera energy response factor was measured using a probe laser coupled to a microjoule meter. The spectral energy transmission of the image relaying system was measured using a grating spectrometer and a calibrated OL-5500 spectral lamp placed at the center of the vacuum chamber.

As noted in Ref. 8, the issues to be addressed in order to obtain a reliable temperature measurement include quality of the sample/window interface, optical properties of the window material, and thermal conduction occurring across the interface. The first two points were thoroughly discussed in a previous letter:[11] (i) the quality of the interface is ensured by electron gun deposition of iron, (ii) we showed that LiF remains transparent up to 2.5 Mbar and inferred its index of refraction. Finally, it was checked that the maximum deviation from iron standard density does not exceed 1%–2% for a thin layer (3 μm). Radiative transfer in the emissive iron layers was also calculated to be negligible, as the optical depth, estimated using a Bloch–Grüneisen scaling,[12] is smaller than any visible wavelength.

Thermal transfer from hot shock-released iron into colder LiF can be calculated using a thermal contact resistance model.[13] We consider that iron's temperature is 20 000 K, which is roughly the highest shock temperature attained in this experiment. In these conditions, the transmitted shock would bring LiF temperature to ≈9000 K according to SESAME equation of state tables.[14] However, we choose to set LiF temperature to 300 K in order to give an upper bound on thermal transfer occurring at the Fe/LiF interface. The nonideal thermal contact between iron and LiF can be represented by an interface of thermal conductivity k_α and width Δx. Its thermal resistance is defined as $r_{\text{th}} = \Delta x / k_\alpha$. Temperature profiles in iron and LiF are given by the heat equation which has the form

$$\frac{\partial^2 T}{\partial x^2} = \frac{1}{D_{\text{th}}} \frac{\partial T}{\partial t},$$

where D_{th} is thermal diffusivity. When the heat exchange is complete, iron and LiF temperatures converge towards a final value T_f given by

$$T_f = T_i^{\text{Fe}} - \frac{T_i^{\text{Fe}} - T_i^{\text{LiF}}}{1+\alpha}, \quad \alpha = \frac{(k\rho C)_{\text{Fe}}}{(k\rho C)_{\text{LiF}}},$$

where T_i^{Fe} and T_i^{LiF} are the initial iron and LiF temperatures and k, ρ, and C denote the thermal conductivities, mass densities, and heat capacities. α was found to be ≈3.5–4.5.[15] This value of α relies on using the Wiedemann–Franz relation for a free electron metal, which is the case for hot liquid iron. The time dependent heat equation solution for iron can be written as

$$T^{\text{Fe}}(t) = T_f + (T_i^{\text{Fe}} - T_i^{\text{LiF}}) \exp(t/\tau) \text{erfc}(\sqrt{t/\tau}),$$

where τ is a temporal parameter given by $\tau = (k r_{\text{th}})^2 / [D_{\text{th}}(1+\alpha)^2]$. τ was measured to be ≈250 ns (Ref. 16) and $n_{\text{th}} \approx 10^{-3}$ cm^2 K/W (Ref. 17) for Fe/sapphire targets. No measurement for τ in the case of Fe/LiF targets has been found in the literature, but we deduce from standard data that τ

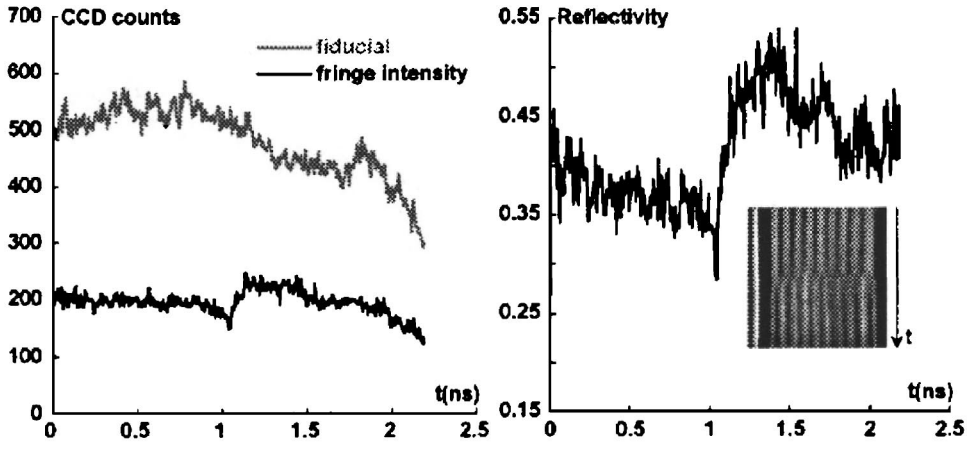

FIG. 2. Absolute reflectivity determination using fiducial and fringe intensity signals. Inset shows corresponding VISAR image.

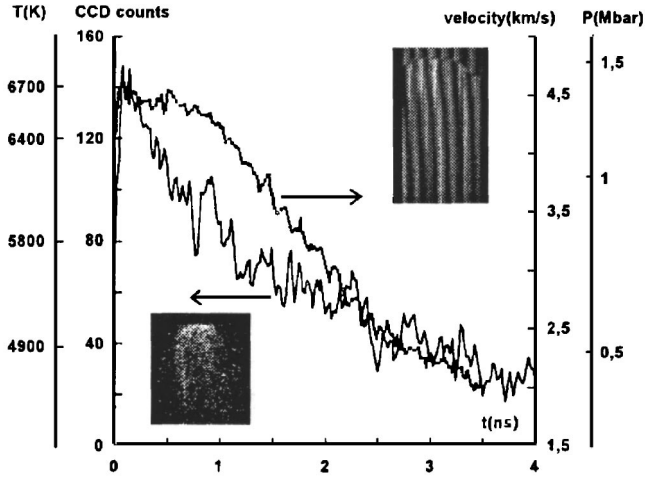

FIG. 3. Simultaneous time-resolved interface velocity (thick dotted line) and self-emission (thin continuous line) signals. Insets show corresponding VISAR (top) and self-emission (bottom) streaked images. Laser intensity is 1.1×10^{13} W/cm^2.

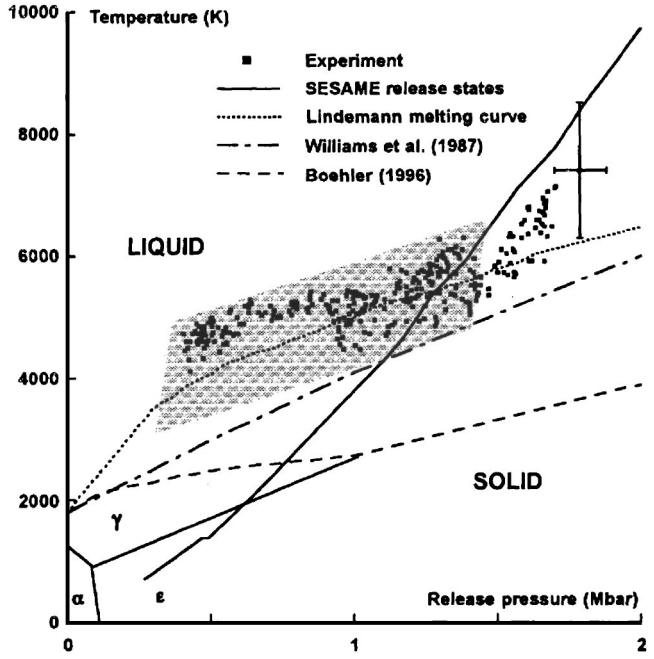

FIG. 4. Iron phase diagram from previous studies and measured temperature at partial release in LiF. Error bar on temperature is dominated by the uncertainty of the absolute energy calibration factor of the system. Shaded area represents experimentally determined melting line locus.

should be smaller in our case. In order to give an upper bound on thermal transfer for Fe/LiF targets, we set $\tau = 100$ ns and $r_{\text{th}}=10^{-3}$ cm^2 K/W. We thus find a final temperature $T_f=16\,060$ K, which is 20% smaller than the initial temperature. However, because of the very short time recording system (<10 ns) of our experiment, iron temperature is found to decrease by means of thermal conduction by less than 4% of its initial value. That is of course true under the hypothesis that the shock is maintained constant during the time of acquisition, which is not completely fulfilled, as the actual shock is decaying. This means that in our conditions, thermal transfer is even less important than the rough estimation we just made and therefore can be neglected.

For several shots, we obtained reliable simultaneous time-resolved velocity and self-emission profiles from which temperature-pressure data points in iron phase diagram were plotted showing a relatively weak scatter (Fig. 3).

Time-resolved data were obtained on shots for which release pressure is $\leqslant$1.8 Mbar. Errors are dominated by the uncertainty of the absolute calibration of the system and are of the order ±15%. Results show that as the shock decays in LiF, temperature is in good agreement with SESAME tables for pressures from 2 to 1.5 Mbar. However when the pressure decreases furthermore to 0.5 Mbar, we find a much weaker slope (Fig. 4).

The small temperature change over a wide pressure range can be attributed to the crossing of iron melting line, as it is consistent with a Lindemann[18] law:

$$T_m = T_m^0\left(\frac{\rho_0}{\rho}\right)^{2/3}\exp\left(2\gamma\left(1-\frac{\rho_0}{\rho}\right)\right)$$

where T_m, ρ, and γ denote melting temperature, mass density, and Grüneisen parameter, respectively. Subscript 0 stands for standard initial state. γ was estimated to vary between 1.7 to 2.5,[5] but the best agreement in our experiment is found for $\gamma=2,5$.

For higher laser intensities, release pressure exceeds 2.5 Mbar and LiF becomes highly absorbing, so that only the initial VISAR fringe shift can be detected. However, fringes time of extinction τ_e allows a direct measurement of compressed LiF absorption coefficient α_{LiB}.

Indeed, the decreasing intensity signal I can be fitted to an exponential function and the compressed LiF thickness grows with $D-v$, where D is shock velocity in LiF and v is interface velocity, so that

$$I(t) = I_0 e^{-t/\tau_e} = I_0 e^{-2\alpha_{\text{LiF}}(D-v)t}.$$

The measured self-emission I_a is therefore apparent and is given by $I_a=I_r e^{-\alpha_{\text{LiF}}z}$, where I_r is the actual interface self-emission, z stands for compressed LiF thickness, given by shock velocity in LiF, and α_{LiF} is the absorption coefficient, deduced from the time of extinction of the fringes and estimated to be $\sim10^6$ m^{-1}. Apparent self-emission is then found to differ from the real self-emission by a factor $\approx$2. The error bars for the highest pressures are larger, as an extra ±10% due to the uncertainty on α_{LiF} has to be included. Nevertheless, these data, located in the liquid phase, are found to be in good agreement with SESAME (Fig. 4).

From the initial release temperatures shown in Fig. 4, one can calculate the corresponding shock temperatures using a Mie–Grüneisen relationship:[8]

$$T_s = T_r \exp\left(-\int_{V_0}^{V}\frac{\gamma}{V}dV\right),$$

where the subscripts s and r denote the shocked and released states, respectively and where $\gamma/V=19.6$ from Ref. 5. All of our shock data (Fig. 5) are in the liquid phase, as were the corresponding initial release temperatures. Because of impedance mismatch between iron and LiF, shock temperature differs from release temperature by typically 25%.

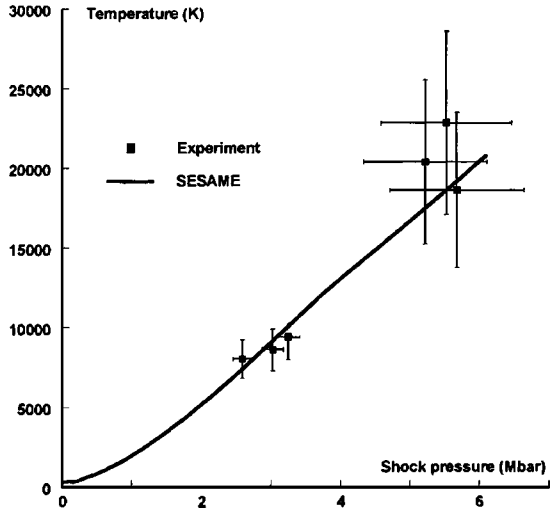

FIG. 5. Iron shock temperature calculated from initial release temperature using Mie–Grüneisen relationship.

The main achievement of this work is to determine experimentally the partially shock-released iron melting curve in the pressure range 0.5–1.5 Mbar, in which temperature varies from 4000 to 5000 K. This challenge was successfully completed using a time-resolved diagnostic allowing simultaneous measurements of interface velocity, reflectivity, and self-emission upon partial release of iron into a LiF window. Extrapolation of our release temperature data along the Lindemann curve yields a melting temperature at inner core–outer core pressure 3.3 Mbar of 7800 ± 1200 K, in good agreement with previous experimental works based on dynamic compression,[7,8] given the error bars. Extrapolation of our melting data to zero pressure is impossible due to the presence of the LiF window which constrains the release pressure to high values.

In this paper, we observed that shock compressed iron seems to melt at higher temperatures than in the static way, using a diamond anvil cell for example. Two possibilities might explain such a discrepancy: (i) metastable superheating and/or (ii) the presence of a solid-solid phase transition around 2 Mbar.

First, it has been qualitatively mentioned that such a discrepancy may result from the very small time scales involved in shock experiments,[19] leading to a thermalized but metastable state as mentioned in Ref. 5. More recently, superheating has been investigated theoretically.[20] In this frame, melting is not described by equating the Gibbs free energy variation to zero. On the contrary, it defines a parameter of melt nucleation rate in solid, which depends on heating rate in K/s. It is then possible to obtain iron solid states at temperatures 25% higher than the melting curve in the case of 10^{12} K/s heating rates, which is typical of shock heating using either gas guns or lasers. Lowering the experimentally measured temperatures by such a quantity could then introduce a better consistency with static results, provided the latter are correct.

Second, recent works[21–23] support the presence of a solid-solid phase transition between 1.5 and 2.5 Mbar that could produce a change of slope of the melting curve and thus provide high melting temperatures.

In order to provide experimental evidence for these possibilities, it is our opinion that the next fulfillment in iron laser-shock experiments is to add an x-ray Bragg diffraction diagnostic probing the presence (or absence) of a crystalline state of compressed iron in the region of interest. Lower temperatures could also be measured using an infrared self-emission diagnostic.

[1] Q. Williams, E. Knittle, and R. Jeanloz, J. Geophys. Res. **96**, 2171 (1991).
[2] E. Knittle and R. Jeanloz, J. Geophys. Res. **96**, 16169 (1991).
[3] R. Boehler, Nature (London) **363**, 534 (1993).
[4] S. K. Saxena, G. Shen, and P. Lazor, Science **264**, 405 (1994).
[5] J. M. Brown and R. G. McQueen, J. Geophys. Res. **91**, 7485 (1986).
[6] J. H. Nguyen and N. C. Holmes, Nature (London) **427**, 339 (2004).
[7] Q. Williams, R. Jeanloz, J. Bass, B. Svendsen, and T. J. Ahrens, Science **236**, 181 (1987).
[8] C. Yoo, N. Holmes, M. Ross, D. Webb, and C. Pike, Phys. Rev. Lett. **70**, 3931 (1993).
[9] R. R. Whitlock and J. S. Wark, Phys. Rev. B **52**, 8 (1995).
[10] L. M. Barker and K. W. Schuler, J. Appl. Phys. **45**, 4789 (1974).
[11] G. Huser, M. Koenig, A. Benuzzi-Mounaix, E. Henry, T. Vinci, B. Faral, M. Tomasini, B. Telaro, and D. Batani, Phys. Plasmas **11**, 61 (2004).
[12] A. N. Gerritsen, *Metallic Conductivity* (Springer, Berlin, 1956).
[13] W. Tang, R. Zhang, F. Jing, and J. Hu, *Shock Compression of Condensed Matter—Seattle 1995* (1996), pp. 279–282.
[14] SESAME, Technical Report LA-UR-92-3407, Los Alamos National Laboratory 1992.
[15] T. J. Ahrens, J. D. Bass, and J. R. Abelson, in *Shock Compression of Condensed Matter—1989*, edited by S. C. Shmidt, J. N. Johnson, and L. W. Davison (Elsevier, New York, 1990).
[16] G. A. Lyzenga and T. J. Ahrens, Rev. Sci. Instrum. **50**, 1421 (1979).
[17] C. Gu, H. Tan, F. Jing, and Q. Gou, *Proceedings of the Second International Symposium on Intense Dynamic Loading and Its Effects*, edited by G. Zhang and S. Huang (Sichuan University Press, 1992), pp. 298–303.
[18] F. A. Lindemann, Phys. Z. **11**, 609 (1910).
[19] R. Boehler, Philos. Trans. R. Soc. London **354**, 1265 (1996).
[20] S. N. Luo and T. J. Ahrens, Appl. Phys. Lett. **82**, 1836 (2003).
[21] J. M. Brown, Geophys. Res. Lett. **28**, 4339 (2001).
[22] T. J. Ahrens, K. G. Holland, and G. Q. Chen, Geophys. Res. Lett. **29**, 54 (2002).
[23] S. N. Luo and T. J. Ahrens, Phys. Earth Planet. Inter. **143–144**, 369 (2004).